Pattern Formation in a Tunable Medium: The Belousov-Zhabotinsky Reaction in an Aerosol OT Microemulsion

Vladimir K. Vanag and Irving R. Epstein

Department of Chemistry and Volen Center for Complex Systems, MS 015, Brandeis University, Waltham, Massachusetts 02454-9110

(Received 12 April 2001; published 7 November 2001)

Turing structures, standing waves, oscillatory clusters, and accelerating waves have been found in the spatially extended Belousov-Zhabotinsky system dispersed in water droplets of a reverse AOT microemulsion. The variety of patterns is determined by the tunable microstructure of the medium, i.e., by the concentration and size of water droplets. We propose a simple model to describe this system.

DOI: 10.1103/PhysRevLett.87.228301 PACS numbers: 82.40.Ck, 02.70.Uu, 68.05.Gh, 82.33.Nq

Pattern formation in reaction-diffusion systems is one of the central themes of modern nonequilibrium science. Turing [1] predicted patterns stationary in time and periodic in space (now generally referred to as Turing patterns), and patterns periodic in both time and space. One realization of the latter patterns associated with an oscillatory instability at finite wavelength is standing waves. The Belousov-Zhabotinsky (BZ) reaction, the catalytic periodic oxidation of malonic acid (MA) by bromate in acidic aqueous solution, is the prototype reaction-diffusion system for generating waves and patterns in such varied media as gels [2], membranes [3], mesoporous glasses [4], and ion-exchange resins [5]. It has become an important model system for various nonlinear processes in biological systems. Until now, neither Turing structures nor standing waves have been observed experimentally in the BZ system. In this Letter we present the first experimental observations and theoretical analysis of pattern formation in the BZ system dispersed in a water-in-oil aerosol OT (AOT) microemulsion (BZ-AOT system) [6,7]. The study of pattern formation in such microheterogeneous media may yield important insights into the development of living systems.

A water-in-oil microemulsion is a thermodynamically stable mixture of water, oil, and surfactant, in which the water and surfactant molecules form spherical, nanometer-size droplets with a polar water core surrounded by a surfactant monolayer. The most widely studied water-in-oil microemulsions employ the surfactant sodium bis(2-ethylhexyl)sulfosuccinate, known as AOT [8]. The radius of water droplet cores is determined [9] by the molecular ratio $\omega = [H_2O]/[AOT]$ and is roughly equal to $R_w = 0.17\omega$ (nm). As the volume fraction ϕ_d of the dispersed phase (water plus surfactant) increases, clusters of droplets begin to appear [10,11]. Percolation occurs when ϕ_d reaches a critical value ϕ_p, leading to a sharp increase of about 3 orders of magnitude in the conductivity [12]. Thus, by varying the composition, one can tune the structural properties of the medium.

Communication between droplets may occur either via exchange with and diffusion through the oil phase or via mass exchange during droplet collision/fusion/fission. Small molecules (e.g., Br_2 or $BrO_2^\bullet$) display very different diffusion coefficients D in the oil and dispersed phases. In the former, D is about the same as the diffusion coefficient of oil molecules, roughly 10^{-5} cm^2/s [13]. For the latter, D is determined by the diffusion of droplets in the oil phase [13] and can be as small as 10^{-7} or 10^{-8} cm^2/s. Reaction-diffusion systems with such different diffusion coefficients possess unusual properties [14–16].

Experiments were carried out under batch conditions at 23 °C. Two stock microemulsions, ME I and ME II, with the same size and concentration of water droplets, were prepared by mixing 1.5 M solutions of AOT in octane with aqueous solutions of H_2SO_4 and malonic acid for ME I and ferroin and bromate for ME II [7]. The reactive microemulsion was generated by mixing equal volumes of the two stock MEs. Microemulsions with different droplet concentrations and the same droplet size were prepared by simple dilution with octane. Most of the reactive microemulsion was used to record bulk oscillations in ferriin absorption at $\lambda = 620$ nm and to measure the electrical conductivity, σ. We found $\sigma < 1$ μS/cm below the percolation threshold and $\sigma > 100$ μS/cm above it.

A small volume of the BZ-AOT mixture was sandwiched between two flat optical windows 50 mm in diameter immediately after mixing the stock MEs. The gap between the windows was determined by the thickness h (= 0.1 mm) of an annular Teflon gasket with inner and outer diameters of 20 and 47 mm, respectively. Patterns could be observed for about 1 h through a microscope equipped with a digital CCD camera connected to a personal computer. The reaction layer was illuminated by a 40 W tungsten source passing through a 450 nm interference filter.

Varying ω, ϕ_d, and $r_0 = \gamma/k'[MA]_0$, where γ is the rate of autocatalytic growth of $[HBrO_2]$ in BZ-AOT ($\gamma = k[H_2SO_4]_0[NaBrO_3]_0^2$, $k = 125$ M^{-3} s^{-1} [17], $k' = 1$ M^{-1} s^{-1}, and subscript 0 signifies initial concentrations in the aqueous phase), we found four major regions in the parameter space (Fig. 1). The bifurcation parameter r_0 characterizes the BZ chemistry, roughly giving the ratio of the rates of the key activation and inhibition steps. At

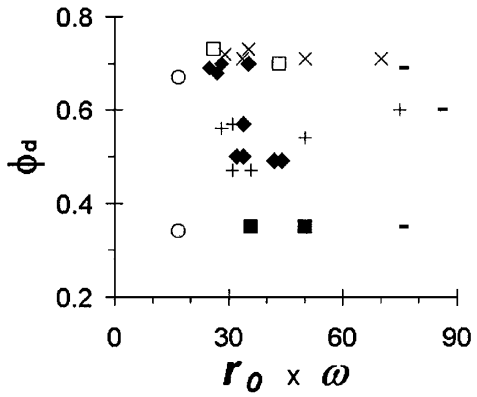

FIG. 1. Dependence of patterns on kinetic ratio r_0 and structural parameters ϕ_d and ω. Symbols: (−) spiral and traveling waves, (■) Turing structures, (◆) standing waves, (□) oscillatory clusters, (+) unusual wave patterns, (×) accelerating waves, and (○) steady state. $[\text{ferroin}]_0 = 4$ mM for all experiments. Coordinates $\omega \times r_0, \phi_d$ give the clearest two-dimensional representation of the results obtained by varying ω, ϕ_d, and r_0. In most experiments, changes in $\omega \times r_0$ are due to changes in r_0 at $\omega = 15$. In all cases, $9 < \omega < 20$.

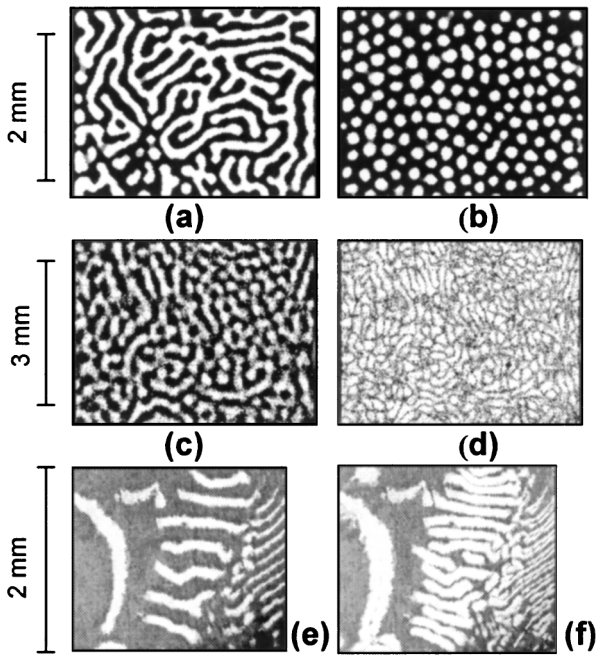

FIG. 2. Patterns in the BZ-AOT system. (a) Labyrinthine Turing structure. $\omega = 15$, $\phi_d = 0.35$. Gray levels quantify [ferroin], with white corresponding to minimum and black to maximum. (b) Hexagonal Turing structure. $\omega = 15$, $\phi_d = 0.35$. (c) Spotlike standing waves. $\omega = 15$, $\phi_d = 0.7$, $T_{\text{bulk}} = 114$ s, period of standing waves $T_{\text{SW}} = 90$ s. (e) Striped standing waves. $\omega = 12$, $\phi_d = 0.5$, $T_{\text{bulk}} = 60$ s, $T_{\text{SW}} = 91$ s. Striped standing waves emerge between traveling waves from the right side and fast phase waves from the left side. (d) [(f)] is a summation of snapshot (c) [(e)] and a snapshot of an antiphase pattern that appears 45 s later. Concentrations (M): $[H_2SO_4]_0 = 0.2$ [(a)–(d)], 0.225 [(e),(f)], $[NaBrO_3]_0 = 0.17$ (a), 0.2 (b), 0.15 [(c)–(f)], and $[MA]_0 = 0.3$ [(a)–(d)], 0.225 [(e),(f)].

high r_0, we obtain traveling or spiral waves like those in the BZ reaction in simple aqueous solution, except that the velocity, v, and wavelength of the BZ-AOT waves are much smaller, about 2–10 μm/s and 0.1–0.3 mm, respectively. Calculating the effective diffusion coefficient D_{eff} of the activator ($HBrO_2$) from the relation $v = 2(\gamma D_{\text{eff}})^{1/2}$ [18], we find that D_{eff} ranges from 10^{-8} to 2×10^{-7} cm^2/s, depending on ω and ϕ_d. A diffusion coefficient of this magnitude is almost certainly associated with the diffusion of water droplets or clusters of droplets in the oil phase.

As we decrease r_0 and approach the boundary between steady state and dynamic behavior (Fig. 1), Turing structures, standing waves, and new types of traveling waves appear. Turing structures emerge at low ϕ_d ($\phi_d < 0.5$) [see Figs. 2(a) and 2(b)], for which bulk oscillations are suppressed in a stirred reactor. They persist for 1 h without changing position. Standing waves [Figs. 2(c)–2(f)] are found at intermediate ϕ_d ($\phi_d = 0.5$–0.7) and, after cessation of bulk oscillations, evolve from traveling waves that form in this initially oscillatory system. The characteristic wavelengths of the Turing structures and standing waves are about 0.18 and 0.23 mm, respectively. Standing waves persist over several tens of oscillation periods, slowly filling the entire medium and finally giving way to the uniform reduced steady state. Standing waves arise most easily near the Teflon gasket, which suggests that zero-flux boundary conditions favor this phenomenon. To our knowledge, this is the first report of standing waves in a reaction-diffusion system in the absence of global coupling or external periodic perturbation [16,19–21].

At higher ϕ_d, above the percolation threshold, oscillatory clusters and accelerating waves occur. Waves [see Figs. 3(a)–3(e)] speed up as they approach the open area left by the collision and subsequent perpendicular departure of the previous pair of waves. The velocity of the waves rises from a low $[\sim(\gamma D_d)^{1/2}]$ to a high $[\sim(\gamma D_{\text{oil}})^{1/2}]$ value. As the waves approach each other, a white bridge appears between the closest points of the approaching waves. Before collision, waves with higher positive local curvature $1/r$ propagate faster, contrary to the eikonal equation [22], $v = v_0 - (1/r)D$, where v_0 is the velocity of a planar front. Such behavior suggests a strong dispersion dependence of the wave velocity on the wavelength [23]. At the same high ϕ_d, but in other regions of the reactor near the boundary, oscillatory standing clusters arise [Figs. 3(f) and 3(g)]. The positions of the nodal lines remain fixed for many cycles. Clusters resemble standing waves, but do not possess an intrinsic wavelength [20].

The dependence of the patterns on ϕ_d can be understood in terms of the variation of the diffusion coefficients of water, D_w, surfactant, D_s, and oil molecules, D_{oil}, with ϕ_d [13]. At small ϕ_d ($\phi_d < \phi_p$, $\phi_p = 0.4$–0.6), D_{oil}/D_w varies from 10 to 100 or more. In this region, $D_w \cong D_s$ is equal to the diffusion coefficient of water droplets, D_d,

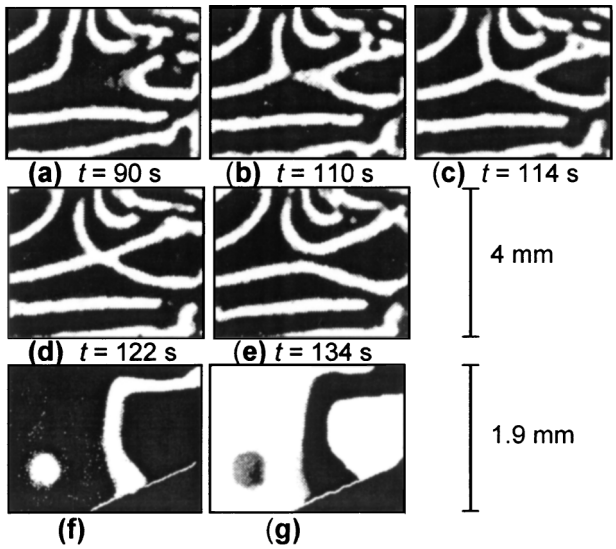

FIG. 3. Patterns in the BZ-AOT system. (a)–(e) Accelerating waves. $\omega = 18.8$, $\phi_d = 0.74$. (f),(g) Oscillatory clusters. $\omega = 13$, $\phi_d = 0.71$, $T_{\text{bulk}} = 105$ s, period of cluster oscillations $T_{\text{cl}} = 109$ s. The black zone in the bottom right corner separated by a light line is the Teflon gasket. The time interval between antiphase snapshots (f) and (g) is 54 s. Concentrations (M): $[H_2SO_4]_0 = 0.2$ [(a)–(g)], $[NaBrO_3]_0 = 0.15$ [(a)–(e)], 0.2 [(f),(g)], and $[MA]_0 = 0.3$ [(a)–(g)].

which is given by $D_d = D_{d0}(1 - \alpha\phi_d)$, where α is positive. As ϕ_d is increased, the ratio D_{oil}/D_w reaches a maximum at the onset of percolation and then begins to decrease toward 1 as a result of the formation of dynamical water channels through which water molecules can travel as fast as oil molecules in the continuous oil phase, while D_s remains small.

The observation of accelerating waves suggests that an activator may diffuse rapidly in the oil phase. In this case, its concentration in the region between two approaching waves is elevated, leading to autocatalysis, which would give rise to a bridge between the waves [Figs. 3(b) and 3(c)]. Among the autocatalytic species, $BrO_2^\bullet$ and $HBrO_2$, bromine dioxide is the more likely candidate. It should dissolve easily in the oil phase, while $HBrO_2$ is polar and should be much less soluble in hydrocarbons. We have added to the well-known Oregonator model [24] two overall reactions:

$$X \rightarrow S, \qquad \text{rate constant} = k_f\,,$$

$$S \rightarrow X, \qquad \text{rate constant} = k_b\,,$$

where $X = HBrO_2$ in the aqueous phase and S represents $BrO_2^\bullet$ (or the product of radical recombination, Br_2O_4) in the oil phase. The forward reaction (k_f) is a combination of $BrO_2^\bullet$ production from $HBrO_2$ and $HBrO_3$ and interfacial transfer. The back reaction (k_b) is a combination of interfacial transfer and the reaction of $BrO_2^\bullet$ with ferroin to yield $HBrO_2$. Thus, there are two activator species in our model, X (active) and S (inactive), with small (D_d) and large (D_{oil}) diffusion coefficients, respectively.

The observation of Turing structures suggests that the inhibitor ($Y = Br^-$) or some species ($Z =$ ferriin or Br_2) that produces the inhibitor ($Z + BrMA \rightarrow Br^-$, $Br_2 + H_2O \rightarrow Br^- + HOBr$, $Br_2 + MA \rightarrow Br^-$) also diffuses rapidly [14]. Theoretically, fast diffusion of ferroin is possible, since mass exchange between water droplets is much faster for species such as ferroin that are more soluble in the surfactant layer than in the water core [25]. However, we have no direct experimental evidence for this idea. Fast diffusion of Br_2 in the oil phase seems more likely, but direct incorporation of Br_2 into a model is difficult. Instead, we assume rapid diffusion of ferriin with a diffusion coefficient intermediate between those for water droplets and Br_2 in the oil phase. The model equations for the bulk concentrations in BZ-AOT microemulsion are then

$$\partial x/\partial t = -k_1xy + k_2y - 2k_3x^2 + k_4x - k_fx + k_b\phi s + d_x\Delta x\,, \tag{1}$$

$$\partial y/\partial t = -k_1xy - k_2y + hk_6z + d_y\Delta y\,, \tag{2}$$

$$\partial z/\partial t = 2k_4x - k_6z - k_5z + d_z\Delta z\,, \tag{3}$$

$$\partial s/\partial t = k_fx/\phi - k_bs + d_s\Delta s\,, \tag{4}$$

where $x = [HBrO_2]_w\phi_w$, $y = [Br^-]_w\phi_w$, $z = [\text{ferriin}]_w\phi_w$, $s = [S]_{\text{oil}}(1 - \phi_d)$, $k_1 = k_1'/\phi_w$, $k_3 = k_3'/\phi_w$, $\phi = \phi_w/(1 - \phi_d)$, and the subscript w signifies water. The diffusion coefficients are normalized so that, with nondimensionalized spatial coordinates, $d = 1\ s^{-1}$ corresponds to $D = 10^{-5}\ cm^2/s$.

Equations (1)–(4) possess only one spatially uniform steady state, the stability of which we have analyzed by linear stability analysis. If the Jacobian matrix has two real, negative eigenvalues and one pair of complex eigenvalues λ_k with positive real part, $\text{Re}(\lambda_k)$, for some k, then the steady state is unstable, and standing waves can arise. If all eigenvalues are real [$\text{Im}(\lambda_k) \equiv \omega_k = 0$, note that ω_k and ω have different meanings] and one is positive for some $k \neq 0$, Turing structures appear. Such behavior is shown in Fig. 4(a).

Figure 4(a) mimics the changes in ϕ_d. At small ϕ_d, when $D_{\text{oil}}/D_w \cong 10$, there is a positive Turing peak $\{\max[\text{Re}(\lambda_k)] > 0\}$ at $\omega_k = 0$ (curve 1). At higher ϕ_d, when $D_{\text{oil}}/D_w \cong 100$, positive $\text{Re}(\lambda_k)$ appear at $\omega_k > 0$ (curve 2), with wave numbers k smaller than that for the Turing peak, i.e., the wavelength of standing waves is larger than that of Turing structures, as seen in our experiments. A small increase in k_b (due to the percolation transition or a boundary effect) leads to the disappearance of wave instability (curve 3) and the emergence of oscillatory clusters or accelerating waves at higher ϕ_d. Far above the percolation threshold, when $d_x = d_y = d_z = d_s$, there is no positive $\text{Re}(\lambda_k)$. Since many of the rate constants for the BZ-AOT system are unknown, we varied our parameters over a broad range to test the model. Standing waves and Turing structures

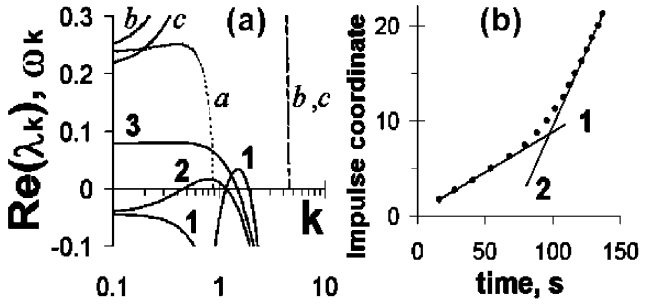

FIG. 4. (a) Dispersion curves for Eqs. (1)–(4). Bold lines 1–3 are $\mathrm{Re}(\lambda_k)$, thin dotted lines $a-c$ are ω_k, with 1 corresponding to a, 2 to b, and 3 to c. $k_1 = 10^5\ \mathrm{M^{-1}\,s^{-1}}$, $k_2 = 0.08\ \mathrm{s^{-1}}$, $k_3 = 200\ \mathrm{M^{-1}\,s^{-1}}$, $k_4 = 2\ \mathrm{s^{-1}}$, $k_5 = k_6 = 0.5\ \mathrm{s^{-1}}$, $h = 1$, $k_f = 1\ \mathrm{s^{-1}}$, $\phi = 1$ (results are independent of ϕ), $k_b\ (\mathrm{s^{-1}}) = 1\ (1, 2), 1.5\ (3)$, $d_s = 1\ \mathrm{s^{-1}}$, $d_x = d_y = d_z/5\ (\mathrm{s^{-1}}) = 0.1\ (1), 0.01\ (2, 3)$. (b) Propagation of accelerating impulse (dots); $k_1 = 6.4 \times 10^4\ \mathrm{M^{-1}\,s^{-1}}$, $k_2 = 0.008\ \mathrm{s^{-1}}$, $k_3 = 400\ \mathrm{M^{-1}\,s^{-1}}$, $k_4 = 1\ \mathrm{s^{-1}}$, $k_5 = 0.005\ \mathrm{s^{-1}}$, $k_6 = 0.015\ \mathrm{s^{-1}}$, $h = 2.5$, $k_f = k_b = 0.2\ \mathrm{s^{-1}}$, $d_x = d_y = d_z = 0.01\ \mathrm{s^{-1}}$, $d_s = 1\ \mathrm{s^{-1}}$, $y_0/y_{\mathrm{SS}} = 20$. Curves 1 and 2 are linear trend lines for initial and final stages.

are found over a wide domain of rate constants and their ratios.

We have simulated Eqs. (1)–(4) numerically in one and two spatial dimensions and have obtained Turing and standing wave patterns similar to those found in our experiments. Our 2D simulations of standing waves reveal that the nodal lines are not stationary. The shape of the oscillatory patterns slowly changes with time, though the characteristic wavelength remains constant. Simulations of accelerating waves in an excitable 1D system are shown in Fig. 4(b). A small region near the left boundary was perturbed to initiate a traveling impulse. In this region $y_0 \cong 0$ and $x_0 \gg x_{\mathrm{SS}}$, in the other regions $y_0 > y_{\mathrm{SS}}$ and $x_0 = x_{\mathrm{SS}}$, and $z_0 = z_{\mathrm{SS}}$ and $s_0 = s_{\mathrm{SS}}$ everywhere; subscripts SS and 0 signify steady state and initial concentrations, respectively. If y_0/y_{SS} is not too large, an impulse starts to propagate with minimum velocity $v_{\min}$. As y approaches y_{SS} in the unperturbed region, the wave velocity increases and reaches $v_{\max}$. The ratio $v_{\max}/v_{\min}$ in general depends upon k_f, k_b, $(d_s/d_x)^{1/2}$, and y_0.

It has recently been shown [26] that in a gel the BZ reaction can affect the physical properties of the medium, leading to mechanical oscillations. We have demonstrated that patterns in a BZ microemulsion are strongly dependent on the "tunable" structural properties of the medium. These observations point toward the possibility of new mechanisms of pattern selection based on interactions between "chemistry" and "structure," phenomena that may provide better models of processes in living systems than simple reaction-diffusion systems with constant diffusion coefficients.

We thank A. M. Zhabotinsky for helpful discussions. This work was supported by the Chemistry Division of the National Science Foundation.

[1] A. M. Turing, Philos. Trans. R. Soc. London B **237**, 37 (1952).
[2] T. Yamaguchi, L. Kuhnert, Zs. Nagy-Ungvarai, S. C. Müller, and B. Hess, J. Phys. Chem. **95**, 5831 (1991).
[3] D. Winston, M. Arora, J. Maselko, V. Gáspár, and K. Showalter, Nature (London) **351**, 132 (1991).
[4] T. Amemiya, M. Nakaiwa, T. Ohmori, and T. Yamaguchi, Physica (Amsterdam) **84D**, 103 (1995).
[5] J. Maselko and K. Showalter, Nature (London) **339**, 609 (1989).
[6] D. Balasubramanian and G. A. Rodley, J. Phys. Chem. **92**, 5995 (1988).
[7] V. K. Vanag and I. Hanazaki, J. Phys. Chem. **99**, 6944 (1995).
[8] T. K. De and A. Maitra, Adv. Colloid Interface Sci. **59**, 95 (1995).
[9] M. Kotlarchyk, S. H. Chen, and J. S. Huang, J. Phys. Chem. **86**, 3273 (1982).
[10] M. Almgren and R. Jóhannsson, J. Phys. Chem. **96**, 9512 (1992).
[11] H. Mays, J. Phys. Chem. B **101**, 10 271 (1997).
[12] M. S. Baptista and C. D. Tran, J. Phys. Chem. B **101**, 4209 (1997).
[13] L. J. Schwartz, C. L. DeCiantis, S. Chapman, B. K. Kelley, and J. P. Hornak, Langmuir **15**, 5461 (1999).
[14] P. K. Becker and R. J. Field, J. Phys. Chem. **89**, 118 (1985).
[15] J.-A. Sepulchre and V. I. Krinsky, Chaos **10**, 826 (2000).
[16] A. von Oertzen, H. H. Rotermund, A. S. Mikhailov, and G. Ertl, J. Phys. Chem. B **104**, 3155 (2000).
[17] V. K. Vanag and I. Hanazaki, J. Phys. Chem. **100**, 10 609 (1996).
[18] J. J. Tyson, in *Oscillations and Traveling Waves in Chemical Systems,* edited by R. Field and M. Burger (Wiley, New York, 1985), p. 93.
[19] V. Petrov, Qi. Ouyang, and H. L. Swinney, Nature (London) **388**, 655 (1997).
[20] V. K. Vanag, L. Yang, M. Dolnik, A. M. Zhabotinsky, and I. R. Epstein, Nature (London) **406**, 389 (2000).
[21] V. K. Vanag, A. M. Zhabotinsky, and I. R. Epstein, Phys. Rev. Lett. **86**, 552 (2001).
[22] V. S. Zykov, Biophysics **25**, 906 (1980).
[23] M. Wellner and A. M. Pertsov, Phys. Rev. E **55**, 7656 (1997).
[24] R. J. Field and R. M. Noyes, J. Chem. Phys. **60**, 1877 (1974).
[25] M. V. Genkin, I. V. Logunov, R. M. Davydov, and O. V. Krylov, Kinet. Catal. **32**, 296 (1991).
[26] R. Yoshida, M. Tanaka, S. Onodera, T. Yamaguchi, and E. Kokufuta, J. Phys. Chem. A **104**, 7549 (2000).